DOI: 10.1002/chem.200500729

Proton- and Redox-Controlled Switching of Photo- and Electrochemiluminescence in Thiophenyl-Substituted Boron–Dipyrromethene Dyes

Holger Röhr,[a, c] Christian Trieflinger,[b] Knut Rurack,*[a] and Jörg Daub*[b]

Abstract: A luminescent molecular switch in which the active thiol/disulfide switching element is attached to a *meso*-phenyl-substituted boron–dipyrromethene (BDP) chromophore as the signalling unit is presented. The combination of these two functional units offers great versatility for multimodal switching of luminescence: 1) deprotonation/protonation of the thiol/thiolate moiety allows the highly fluorescent *meso-p*-thiophenol-BDP and its nonfluorescent thiolate analogue to be chemically and reversibly interconverted, 2) electrochemical oxidation of the monomeric dyes yields the fluorescent disulfide-bridged bichromophoric dimer, also in a fully reversible process, and 3) besides conventional photoexcitation, the well separated redox potentials of the BDP also allow the excited BDP state to be generated electrochemically (i.e., processes 1) and 2) can be employed to control both photo- and electrochemiluminescence (ECL) of the BDP). The paper introduces and characterizes the various states of the switch and discusses the underlying mechanisms. Investigation of the *ortho* analogue of the dimer provided insight into potential chromophore–chromophore interactions in such bichromophoric architectures in both the ground and the excited state. Comparison of the optical and redox properties of the two disulfide dimers further revealed structural requirements both for redox switches and for ECL-active molecular ensembles. By employing thiol/disulfide switching chemistry and BDP luminescence features, it was possible to create a prototype molecular ensemble that shows both fully reversible proton- and redox-gated electrochemiluminescence.

Keywords: boron–dipyrromethene · electrochemiluminescence · fluorescence · molecular switches · redox chemistry · thiol/disulfide chemistry

Introduction

The development of functional molecules capable of performing chemically or physically controlled actions and reporting on or transducing these through luminescence signals has attracted considerable attention in recent years. Employment of luminescence as the technique with which to access such information harbours the advantages of being nondestructive, noninvasive and sensitive, and offers remote access to a generated optical event. Examples of functional supramolecular systems communicating through luminescence include molecular-scale sensors,[1] switches,[2] "logic gates",[3] motors and machines,[4] wires,[5] or arrays, cascades and cassettes that operate through energy- or electron-transfer processes.[6] Besides the constant motivation to improve the features that govern the performance of such systems in terms of efficiency, functional supramolecules that can be addressed or controlled through two or more different inputs while delivering an optical output signal have recently focussed research efforts. Such advanced architectures allow independent control of the various states of the system and can be achieved by combinations of, for instance, redox and photochromic units,[7] chemically sensitive and redox units,[8] photochromic and chemically sensitive units[9] or a combination of all the three types of stimuli-responsive actions.[10]

A particularly attractive, intrinsically dual-mode switching unit is the thiol group. This simple chemical group can be

[a] Dipl.-Phys. H. Röhr, Dr. K. Rurack
Div. I.3, Bundesanstalt für Materialforschung und -prüfung (BAM)
Richard-Willstätter-Strasse 11, 12489 Berlin (Germany)
Fax: (+49) 30-8104-5005
E-mail: knut.rurack@bam.de

[b] Dr. C. Trieflinger, Prof. J. Daub
Institut für Organische Chemie, Universität Regensburg
Universitätsstrasse 31, 93053 Regensburg (Germany)
Fax: (+49) 941-943-4984
E-mail: joerg.daub@chemie.uni-regensburg.de

[c] Dipl.-Phys. H. Röhr
Associated with: Fachbereich Biologie, Chemie, Pharmazie
Freie Universität Berlin, Takustrasse 3, 14195 Berlin (Germany)

Supporting information for this article is available on the WWW under http://www.chemeurj.org/ or from the author.

deprotonated (i.e., chemically controlled) and can also be oxidized to form disulfide bridges. Both reactions are reversible (i.e., the thiolate can be reprotonated and the disulfide bond can be broken by reduction). Although it is straightforward and versatile in nature, examples of switchable luminescent molecules based on this control unit have, to the best of our knowledge, yet to be reported.[11] This is surprising, as the thiol/disulfide redox pair plays an outstanding role in protein biochemistry, most importantly as redox-active switches through the two oxidation states of glutathione or other cysteine-containing proteins.[12] Moreover, the unravelling of the detailed mechanisms of nature's thiol redox chemistry has experienced significant progress in the last years, basically because redox-active fluorescent tags have become available.[13,14] These have been engineered by attaching cysteine moieties to green fluorescent protein[13] or yellow fluorescent protein.[14] Despite the results of first attempts toward the design of artificial photochromic and fluorescent redox labels for cysteine-containing proteins,[15] thiol/disulfide-active redox switches are assumed to be promising candidates for biomolecular nanoelectronics.[16]

Here we present a simple luminescent molecular switch in which the active thiol/disulfide element is attached to a *meso*-phenyl-substituted boron–dipyrromethene (BDP) chromophore as the signalling unit. BDP dyes possess valuable spectroscopic features, such as intense absorption ($\varepsilon > 80\,000\,\mathrm{M}^{-1}\mathrm{cm}^{-1}$) and emission ($\Phi_f > 0.70$) bands in the visible spectral range above 500 nm.[17] These dyes are readily soluble in a large variety of solvents of different polarity, and tuning of their spectroscopic properties towards the near infrared region is facile.[8a,18] If they contain an appropriate unit—especially in the *meso*-position—that is either redox-active or sensitive toward chemical inputs, such dyes can show exceptionally powerful switching features, commonly manifested in dramatic changes in fluorescence intensity or lifetime.[19,20] The combination of thiol/disulfide chemistry and BDP photophysics thus promised distinct ON/OFF behaviour through simple and rapid adjustment and interconversion of the chemical or physical states of the active control unit. Moreover, since the BDPs' green emission of high brightness can be generated not only photochemically but also electrochemically,[8c,21] another stimulus for the research reported here was the construction of a prototype molecular system capable of displaying chemically and redox-modulated electrochemiluminescence (ECL).

The thiophenyl-substituted BDP derivatives we studied in this work are illustrated here. Compounds *p*SH-**1** and (*p*S-

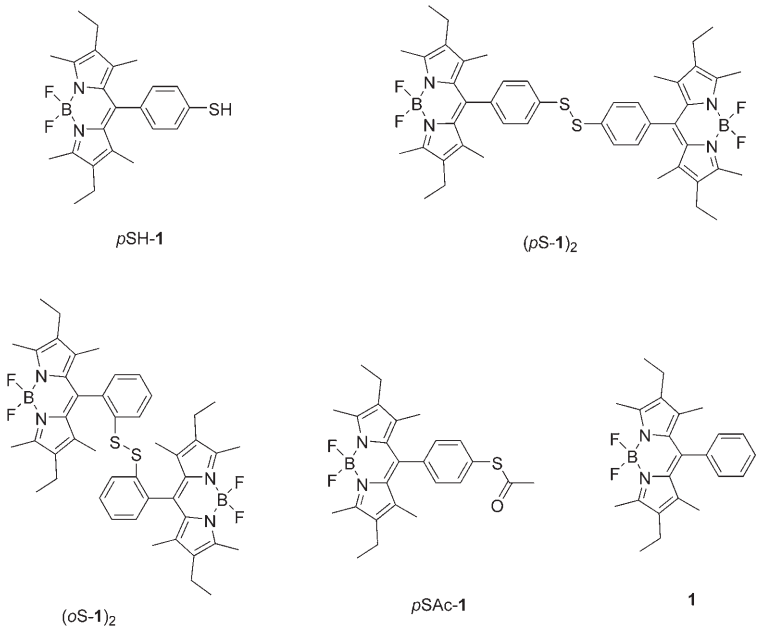

Abstract in German: *In dieser Arbeit wird ein lumineszierender molekularer Schalter vorgestellt, bei dem das aktive Thiol/Disulfid-Schaltelement an einen meso-phenylsubstituierten Bordipyrromethen (BDP) Farbstoff als Signal gebende Komponente gekoppelt ist. Die Kombination dieser beiden funktionellen Einheiten offeriert eine hohe Vielseitigkeit für das multimodale Schalten der Lumineszenz: 1) die Deprotonierung/Protonierung der Thiol/Thiolat-Gruppe erlaubt es, das stark fluoreszierende meso-p-Thiophenol-BDP und das analoge, nicht fluoreszierende Thiolat chemisch reversibel ineinander zu überführen, 2) die elektrochemische Oxidation der monomeren Farbstoffe ergibt das fluoreszierende, disulfidverbrückte, bichromophore Dimer—dieser Prozess ist ebenfalls vollständig reversibel, und 3) neben der konventionellen Anregung mit Licht erlauben die deutlich getrennten Redoxpotenziale des BDPs ebenfalls eine elektrochemische Generierung des angeregten BDP-Zustandes, d.h., Prozesse 1) und 2) können dazu eingesetzt werden, sowohl die Photo- als auch die Elektrochemilumineszenz (ECL) des BDP zu steuern. Diese Arbeit stellt die Charakteristika der verschiedenen Zustände des Schalters vor und diskutiert die zu Grunde liegenden Mechanismen. Die Untersuchung des ortho-Analogen des Dimers vermittelte zudem Einsicht in mögliche Chromophor–Chromophor-Wechselwirkungen im Grund- wie im angeregten Zustand von solchen bichromophoren Architekturen. Der Vergleich der optischen und Redoxeigenschaften der beiden Disulfid-Dimere gab des Weiteren Aufschluss über strukturelle Voraussetzungen von Redoxschaltern sowie ECL-aktiven molekularen Ensembles. Unter Einsatz schaltbarer Thiol/Disulfid-Chemie und mit den Lumineszenzeigenschaften der BDPs war es möglich, ein erstes molekulares Ensemble zu entwickeln, das vollständig reversible protonen- als auch redoxgesteuerte Elektrochemilumineszenz zeigt.*

1)$_2$ were designed as the principle redox pair for multimode switching of fluorescence and ECL, and the main intention of this paper is to characterize and demonstrate the versatility of the system. To achieve better understanding of the structural features of such compounds, the structurally more demanding twin (*o*S-**1**)$_2$ was also synthesized and investigated. With recent advances in protein labelling through thiol functions[22] and the according future potential of *p*SH-**1** to act as a redox-active fluorescent tag in biosensory chemistry, a comparative study of (*p*S-**1**)$_2$ and (*o*S-**1**)$_2$ also promised insight into possible interchromophore interaction. These might play an important role if, for instance, two BDP labels were to come into close contact in a hydrophobic pocket or on the surface of a protein, as recently shown by Bergström et al.[23]

Results and Discussion

Synthesis: The BDP-appended disulfide (*p*S-**1**)$_2$ was obtained from 4,4′-dithiobisbenzoic acid by conventional BDP synthesis procedures (Scheme 1 A),[10a] via in situ formation of the acid chloride, while (*o*S-**1**)$_2$ was prepared in a similar way from 2,2′-dithiobisbenzoic acid. Reduction of (*p*S-**1**)$_2$ afforded *p*SH-**1** in 50% yield (Scheme 1 A).[24] The synthesis of reference compound *p*SAc-**1** is depicted in Scheme 1 B.

Absorption and fluorescence spectroscopy: The *para*- and *ortho*-thiophenyl-substituted BDPs were investigated both by absorption and by steady-state and time-resolved fluorimetry in their oxidized disulfide and reduced thiol forms in a variety of solvents covering a large polarity range (from hexane to DMSO). Compounds *p*SAc-**1** and **1** were included in the studies as models.

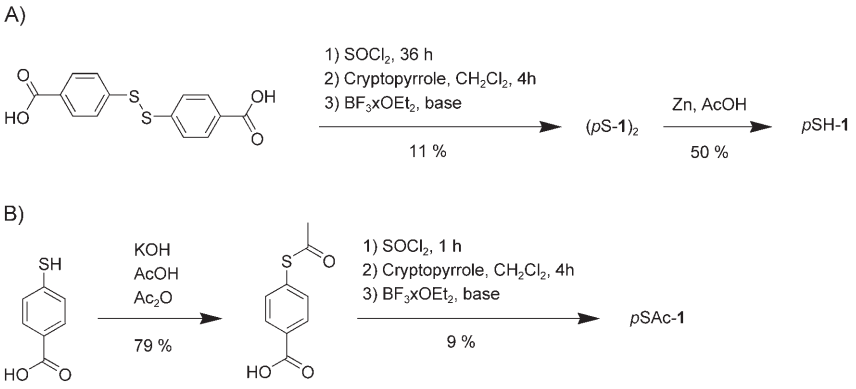

Scheme 1. A) Synthetic route to (*p*S-**1**)$_2$ and *p*SH-**1**. B) Synthetic route to *p*SAc-**1**.

Independent of solvent polarity, the absorption maxima of *p*SH-**1**, (*p*S-**1**)$_2$, *p*SAc-**1** and **1** show typical BDP features and are centred at 525 ± 2 nm (Figure 1). The absorption spectra of (*o*S-**1**)$_2$ possess similar shapes and are slightly red-shifted by 5 nm. These negligible differences indicate strong

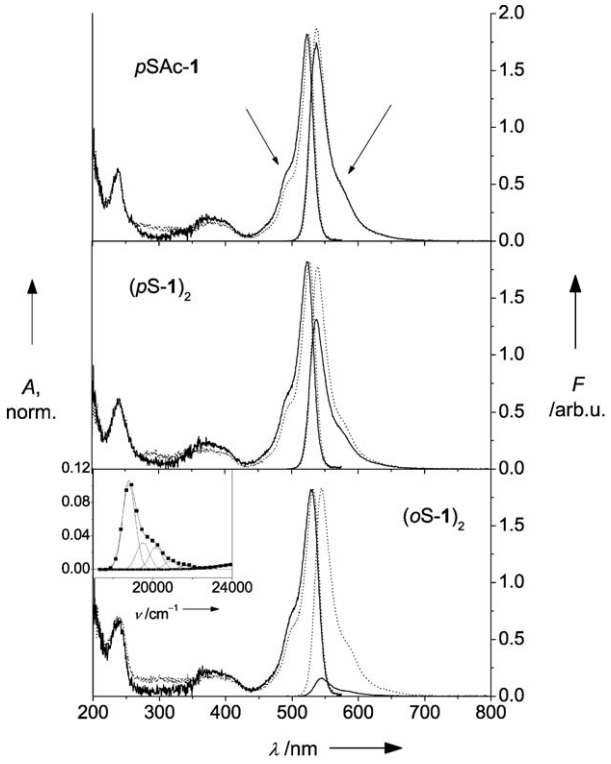

Figure 1. Normalized absorption and relative fluorescence spectra of *p*SAc-**1** (top), (*p*S-**1**)$_2$ (middle) and (*o*S-**1**)$_2$ (bottom) in MeCN (solid line) and hexane (dotted line). The characteristic shoulders in the spectra are due to the C–C frame vibration indicated by the arrows in the top panel. Inset: Lowest-energy absorption band of (*o*S-**1**)$_2$ in hexane converted to the energy scale and results of the spectral deconvolution procedure.

internal decoupling of the chromophoric subunits (BDP and phenyl moieties) and thus the weak influence of the presence or absence of *para*- or *ortho*-substituents. The full widths at half-maximum (*fwhm*s) of the typical BDP bands are virtually identical for all the dyes, slightly increasing from—for instance—ca. 740 cm^{-1} in hexane to ca. 790 cm^{-1} in DMSO for (*p*S-**1**)$_2$ and *p*SAc-**1** and from 740 to 820 cm^{-1} in the two solvents for (*o*S-**1**)$_2$. Besides these characteristics, the cyanine-type nature of the BDP chromophore is further manifested in the molecular C-C frame vibration typical of cyanine dyes[25] at ca. 1300 cm^{-1} and denoted by arrows in Figure 1. These characteristic features of BDP dyes have recently also been found by us for more extended BDP-type π systems.[18b] The molar absorptivities support the presence of two independent BDP moieties in the dimers (i.e., $\varepsilon_{max} \approx 60\,000\,M^{-1}cm^{-1}$ for *p*SH-**1** in all the solvents studied and $\varepsilon_{max} \approx 119\,000\,M^{-1}cm^{-1}$ and $102\,000\,M^{-1}cm^{-1}$

for (pS-**1**)$_2$ and (oS-**1**)$_2$, respectively). The steady-state emission features are consistent with these observations. The typical BDP emission of mirror-image shape is observed in all cases, with maxima occurring at 538 ± 2 nm for pSH-**1**, (pS-**1**)$_2$, pSAc-**1** and **1** and at 546 ± 2 nm for (oS-**1**)$_2$. Moreover, the emission bands show *fwhm*s identical to those of the absorption data within $\pm10\,cm^{-1}$. No dual fluorescence was observed during these studies, indicating the absence of the formation of emissive charge-transfer states.[17b,18b,26]

With respect to pSH-**1**, these findings are consistent with our previous report on a *meso*-(4-hydroxyphenyl)-substituted BDP in reference [27]. This analogue, with an OH group instead of the SH group in pSH-**1**, also shows bright fluorescence with the typical BDP characteristics in its undissociated state in various solvents. While these straightforward spectral characteristics are favourable for the facile operation of an optical switching system, what is essential for the performance of a proton- and redox-active fluorescent switch is controlled ON/OFF behaviour of the distinct switching states. Ideally, in a two-state system, these states should show dramatic differences in their fluorescence intensities. In accordance with the work reported in reference [27], we found similar behaviour for pSH-**1** and its deprotonated form pS-**1**$^-$.[28] Whereas the former, for instance, emits green fluorescence with a high quantum yield comparable to that of the model compound pSAc-**1** (Table 1), the latter is virtually nonfluorescent. The distinctly higher donor strength of the thiolate group obviously opens up an efficient quenching pathway, most probably through rapid back-electron transfer with charge-shift nature. Such nonradiative transitions to the ground state are well known for ionic dye systems.[29] In the present case, preliminary quantum chemical calculations at semiempirical level[30] suggest that deprotonation might result in a certain degree of planarization of the entire chromophore, exemplified by a reduction in the interannular twist angle θ^{calcd} from 89° in pSH-**1** to 55° in pS-**1**$^-$. This conformational effect might then give rise to an oscillator-weak charge-transfer (CT) transition, located at the low-energy side of the intense BDP band.[31] The spectroelectrochemical measurements reported below indeed support such an assumption, as a weak shoulder appears in the region around 570 nm during the first reduction step of (pS-**1**)$_2$ where pS-**1**$^-$ is formed (see left panel of Figure 4 and Scheme 4; changes similar to those in the left panel of Figure 4 were also observed during the titration of pSH-**1** with base). Deactivation of an ionic CT state then most probably proceeds in radiationless fashion by the described charge-shift mechanism. Furthermore, in the current system, the fluorescence could be reversibly switched OFF and ON by successive addition of base (e.g., 1,8-diazabicyclo[5.4.0]undec-7-ene, DBU) and acid (e.g. trifluoroacetic acid, TFA), respectively. The proton-induced action is further confirmed by the fact that (pS-**1**)$_2$ and pSAc-**1** do not show any spectroscopic changes upon base addition.

For the goal of redox control over the switching features of pSH-**1**, the fluorescence output of the oxidized disulfide dimer (pS-**1**)$_2$ is also important, as it presents the third cornerstone in the cycle (Scheme 2). The data for the dimer are included in Table 1. It is apparent that (pS-**1**)$_2$ shows considerable fluorescence with the typical BDP features in solvents of any polarity, suggesting that the phenyl–disulfide–phenyl bridge is large enough to prevent inter-BDP chromophore communication. Results obtained recently by Wang et al. on symmetric disulfide triads with the same spacer and two naphthalimidyl fragments as chromophores support our observations.[32] Nonetheless, the fluorescence quantum yield of (pS-**1**)$_2$ is reduced in relation to pSH-**1**, which is conceivable in view of the higher donor potential of the sulfur atom in the latter compound.

For a three-state switch as shown in Scheme 2, with pSH-**1** and pS-**1**$^-$ as the proton-addressable and (pS-**1**)$_2$ as the additional redox partners, the moderately diminished fluorescence of the oxidized compound in relation to the reduced form is important. In particular, the different fluorescence

Table 1. Spectroscopic data for the compounds studied in selected solvents at 298 K; for additional data see Table S1 in the Supporting Information.

Compound	Solvent	λ_{abs}(max) [nm]	λ_{em}(max) [nm]	Φ_f	τ_f [ns]
pSH-**1**[a]	MeCN	522	536	0.64	4.72
pS-**1**$^-$[a]	MeCN	518	n.d[b]	$<10^{-4}$	[c]
(pS-**1**)$_2$	MeCN	524	537	0.52[d]	3.44[d]
	THF	526	539	0.72	4.17
	hexane	527	539	0.67	3.78
(oS-**1**)$_2$	MeCN	530	544	0.067	[e]
	THF	533	547	0.73	[e]
	hexane	532	545	0.78	[e]
pSAc-**1**	MeCN	523	537	0.72	4.68
	THF	526	539	0.72	4.11
	hexane	526	538	0.73	4.02
1	MeCN	521	535	0.87	5.25
	hexane	524	537	0.82	4.77

[a] Measured only in degassed MeCN, because of rapid autooxidation in the presence of air. [b] Not determined. [c] <3 ps. [d] Virtually identical in degassed MeCN. [e] See description in the text and data in Table 2.

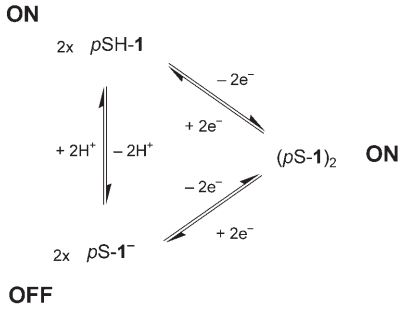

Scheme 2. Illustration of the switching states and processes of the title compounds.

decay times—4.72 ns for *p*SH-**1** and 3.44 ns for $(p\text{S-}\mathbf{1})_2$—make it possible to distinguish between the two forms with any commercial fluorescence lifetime instrumentation that can be operated in the picosecond time domain. All the states of the switch can thus be accessed by simple spectroscopic experiments.

Before we discuss the electrochemical side of the chemically and redox-active switching system, we will remain with the dynamic fluorescence properties of the dimers and compare the behaviour of $(p\text{S-}\mathbf{1})_2$ and $(o\text{S-}\mathbf{1})_2$ in more detail. As mentioned in the Introduction, an important aspect in the use of dyes as fluorescent tags in labelling or imaging applications is the behaviour of the dye under high-loading conditions or under circumstances in which binding sites are situated in close proximity to one another. In both cases, interchromophore communication can arise and can produce either aggregation effects or fluorescence quenching. The latter can be particularly important when such closely located binding sites are contained within a hydrophobic pocket of, for example, a protein, which might then facilitate accommodation and cross-talk of (two) fluorophores. Firstly, it is important to note that we did not observe any other features for concentrated solutions of $(p\text{S-}\mathbf{1})_2$ beyond those reported in Table 1. Secondly, as mentioned above, the spectral characteristics of $(o\text{S-}\mathbf{1})_2$ are virtually identical to those of the other BDPs investigated here.[33] However, the data for $(o\text{S-}\mathbf{1})_2$ in Tables 1 and S1 further reveal that the fluorescence quantum yield decreases as a function of solvent polarity for solvents more polar than THF and that the fluorescence of $(o\text{S-}\mathbf{1})_2$ is considerably lower than that of $(p\text{S-}\mathbf{1})_2$ in solvents of high polarity. Moreover, whereas $(p\text{S-}\mathbf{1})_2$ exhibits single-exponential fluorescence lifetimes throughout the spectrum of solvents studied and $(o\text{S-}\mathbf{1})_2$ largely shows monoexponential fluorescence decay kinetics in apolar solvents, strongly nonexponential decays are found for $(o\text{S-}\mathbf{1})_2$ in all the polar solvents. This concomitant reduction of Φ_f and τ_f—when the latter is expressed as the average lifetime—points to activation of a nonradiative channel as the quenching process rather than a change of the emitting state to one with a lower emissivity. Apparently, whereas weakly polar solvents produce sufficient isolation of both BDP units to prevent any kind of pronounced interaction, in polar solvents fluorescence quenching occurs, most probably through chromophore–chromophore interaction within the dimer. Because the spectral absorption and emission features of $(o\text{S-}\mathbf{1})_2$ are independent of the solvent and remain BDP-like, H- or J-aggregate formation is less likely to be the cause of the quenching. In this case, new bands at the high- or low-energy side of the $S_1 \leftarrow S_0$ band of the BDP spectrum should occur.[23,34]

A closer look at the fluorescence decays of $(o\text{S-}\mathbf{1})_2$ in polar solvents reveals that analysis of the decay traces only yields acceptable fits when three discrete exponentials are employed. Furthermore, these three components are only found as decay times, and their relative amplitudes remain virtually constant when monitored at three different emission wavelengths between 540 and 600 nm, over the entire emission band. To acquire access to the underlying photophysical mechanisms it is important to keep in mind that only the typical BDP emission band is observed (Figure 1) and that these nonexponential decays can thus only be attributed to emitting (monomeric) BDP moieties. However, the occurrence of three distinct excited state species for a bichromophoric molecule seems rather unusual. If we consider further that the formation of intramolecular sandwich-type conformations—presumably preexisting in the ground state—-is possible for $(o\text{S-}\mathbf{1})_2$, it might be helpful to invoke another formalism for the analysis of the fluorescence decays: lifetime distribution analysis (LDA; Figure 2). LDA is based on the assumption that an ensemble of molecular emitters showing a quasicontinuous distribution of lifetimes or reaction rates is present in the solution.[35] In contrast to distinct fluorophores in liquid solution, such an ensemble might constitute of molecules in confined media such as polymers, zeolites, or inclusion complexes in which the microenvironment of the discrete emitters is heterogeneous.[36] Other examples in which this strategy has successfully been applied to recover the decay kinetics include surface-bound fluorophores[37] or flexible bichromophoric systems in which the relative orientation of the two chromophores can vary around one or more certain preferred conformation(s).[38] The molecular structure of $(o\text{S-}\mathbf{1})_2$, which is designed in such a fashion that the two chromophore units can adopt a sandwich-type conformation, indicates that this dye might fall into the latter category (Scheme 3). In LDA of the decays of such systems, the envelope of a lifetime distribution function usually shows several peaks, corresponding to the average lifetimes $<\tau>$ (or centres of gravity) of certain preferred conformations or environmental situations, and each of the peaks is characterized by a specific width σ. The width of the function, then, is a measure of the intramolecular spatial distribution of, or microheterogeneity around, the emitting species.

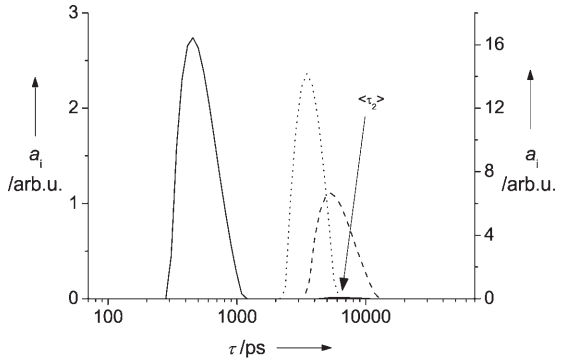

Figure 2. Representative lifetime distribution functions of $(o\text{S-}\mathbf{1})_2$ in DMSO (solid, minor mode indicated by the arrow) and THF (dashed), as well as $(p\text{S-}\mathbf{1})_2$ in MeCN (dotted), obtained for 494/564 nm excitation and emission wavelengths. For data, see Table 2.

The data in Table 2 show two trends. A bimodal distribution with a centre at ca. 0.5 ns and a second centre in the 5–6 ns range, the latter being largely independent of the solvent, is found in the region of high solvent polarity. In the

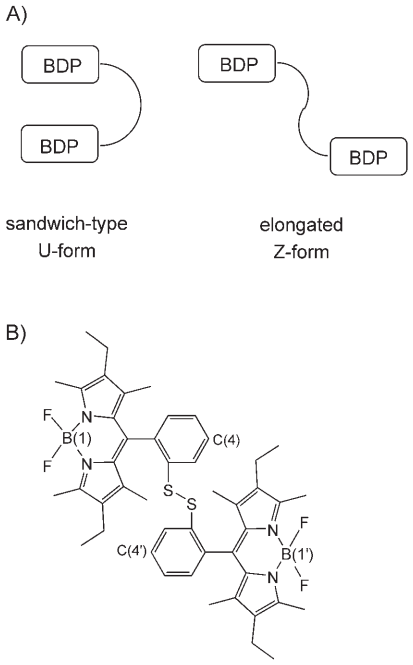

Scheme 3. A) Two possible conformers of $(o\text{S-}\mathbf{1})_2$ with maximum (U-form) and minimum (Z-form) chromophore–chromophore interaction. The apparent torsion angles between atoms B1-C4-C4′-B1′ (see B) obtained for the two stable U- and Z-conformations of $(o\text{S-}\mathbf{1})_2$ by ground-state geometry optimization by the AM1 method are −61° for the U-form and −134° for the Z-form.

Table 2. Fluorescence lifetime data for $(o\text{S-}\mathbf{1})_2$ in various solvents at 298 K; for additional data see Table S2 in the Supporting Information.[a]

Compound	Solvent	$<\tau_1>$ [ns]	$<\tau_2>$ [ns]	φ_2^{rel}[b]
$(o\text{S-}\mathbf{1})_2$	DMSO	5.23 ± 1.00	0.41 ± 0.16	0.64
	MeCN	6.47 ± 0.74	0.49 ± 0.09	0.68
	acetone	3.29 ± 2.35	0.33 ± 0.09	0.06
	THF	5.44 ± 1.52	–	–
	hexane	5.99 ± 1.37	–	–
$(p\text{S-}\mathbf{1})_2$	MeCN	3.41 ± 0.66	–	–
*p*SAc-**1**	MeCN	4.63 ± 0.84	–	–

[a] The data are averages from three independent fits of three decays recorded between 540 and 600 nm for two samples. [b] Relative amplitude of the short decay mode $<\tau_2>$.

weak and medium polar solvents, monomodal distributions are obtained. For the first group of highly polar solvents, the relative contributions of the two modes vary as a function of solvent polarity, reflecting the overall decrease in fluorescence quantum yield: fast decay times predominate in DMSO and MeCN, while slow ones present the major mode in acetone. In the less polar solvents, only the slow decay times are found. For a better illustration, Figure 2 shows representative LDA results for $(o\text{S-}\mathbf{1})_2$ in THF and DMSO. In the less polar solvents, the width of the monomodal distribution of lifetimes of $(o\text{S-}\mathbf{1})_2$ is still considerably broader than that of the corresponding single exponential decays of the *para* analogue $(p\text{S-}\mathbf{1})_2$, as well as model *p*SAc-**1** (Table 2). In accordance with the previously outlined hypothesis of sandwich formation, and due to the lack of rise times, the behaviour of $(o\text{S-}\mathbf{1})_2$ cannot be described in terms of classical exciplex/excimer or charge-transfer formation models, which are often found for bichromophoric compounds, and the involvement of molecular aggregates is also unlikely (vide ante). In contrast, we tentatively attribute these results to certain prearrangements of the molecules already present in the ground state. If we assume that the molecules can adopt folded conformations, such as the U-form, that bring the two BDP moieties into closer proximity, fast intramolecular fluorescence energy transfer can occur upon excitation.[39] Actually, ground-state geometry optimization performed for $(o\text{S-}\mathbf{1})_2$ at the AM1 level converged to two different conformations: the U-shaped, quasi-"sandwich"-type structure and a more Z-shaped conformation that resembles a zigzag analogue of $(p\text{S-}\mathbf{1})_2$ (Scheme 3). The dipole moments of both conformations were calculated to be 6.6 D for the U- and 3.0 D for the Z-form, suggesting that polar solvents might stabilize the U-form better. The efficiency of the quenching process then strongly depends on the mutual preorientation and distance between the two identical fluorophores, with the spatial distribution of the apparent torsion angle around the disulfide bond (see caption of Scheme 3 for definition) in the U-form in particular being able to entail broader lifetime distributions. Furthermore, the bimodality of the distributions in the highly polar solvents suggests that both sets of conformations actually seem to be present and play a role for the reduced fluorescence. Molecules in the Z-form, with a conformation that more closely resembles $(p\text{S-}\mathbf{1})_2$, may thus be responsible for the slow decays of about 5–6 ns, whilst molecules in the U-form—apparently decoupled in the ground state but sufficiently preoriented for interaction in the excited state—would accordingly be responsible for the fast decay times.

Another interesting feature of substituted BDP dyes, the distinctly longer decay times of *ortho*-donor-phenyl substituted compounds in relation to their unsubstituted or *para*-substituted analogues, is also evident from Table 2. Whereas the fluorescence of *p*SAc-**1** decays in 4.68 ns in MeCN, **1** shows a lifetime of 5.25 ns and $(o\text{S-}\mathbf{1})_2$ a lifetime of 6.47 ns. Similar observations have previously been made by us for a 1,1′-binaphthyl-appended bichromophoric BDP[20a] and for 2-methoxy-3-BDP-naphthalene, which show decay times of 6.17 and 6.55 ns in acetonitrile. These features are not yet completely understood, and current theoretical and experimental work is directed at more fundamental understanding. A possible explanation might involve hindered rotation in *ortho*-substituted derivatives, which might suppress a dark deexcitation channel of the BDP chromophore through a "butterfly"-type structure. Lindsey et al. recently postulated that population of such a "dark state" involves coplanarization of the *meso*-substituent with a part of the dipyrromethene ring system.[40,41]

Low-temperature measurements in the time domain at liquid nitrogen temperature yielded single-exponential decays for all the derivatives investigated. Compounds $(p\text{S-}\mathbf{1})_2$ and *p*SAc-**1**, which decay with 4.2 and 4.8 ns lifetimes in

ethanol at 298 K, showed lifetimes of 6.1 and 6.2 ns at 77 K. Furthermore, the bimodal distribution of $(o\text{S-}\mathbf{1})_2$ in methanol at 298 K is not maintained in the glass, in which the dye shows a monoexponential decay with $\tau_f = 7.1$ ns. These results indicate that any dark relaxation pathway that relies on larger molecular motions is closed at 77 K.

Electrochemistry and spectroelectrochemistry: Returning to the redox-active switching process at room temperature, cyclic voltammetry clearly reveals that the thiol/disulfide transition of the BDPs can be performed and controlled electrochemically. Whereas *p*SAc-**1** shows only the typical reversible reduction and quasi-reversible oxidation of the BDP moiety (−1600 mV and +620 mV vs. Fc^+/Fc in MeCN),[42] an additional redox process arises in the cyclic voltammogram of $(p\text{S-}\mathbf{1})_2$, with a reduction at −1545 mV and a significantly displaced back oxidation at −265 mV (Figure 3).[43] As can be shown by calibration against ferrocene, each process represents a two-electron transfer for $(p\text{S-}\mathbf{1})_2$, due to its dimeric structure. The high similarity of the UV/Vis spectra of reduced $(p\text{S-}\mathbf{1})_2$ obtained in spectroelectrochemical measurements (Figure 4) and of $p\text{S-}\mathbf{1}^-$, obtained by deprotonation of *p*SH-**1**, strongly supports the attribution of the first reduction step at −1545 mV to a dissociative conversion of $(p\text{S-}\mathbf{1})_2$ into two molecules of $p\text{S-}\mathbf{1}^-$ [electron transfer–chemical step–electron transfer (or ECE) mechanism; vide infra],[44,45] which is electrochemically reversed at −265 mV. As $p\text{S-}\mathbf{1}^-$ is nonfluorescent, the ON and OFF positions of the fluorescent switch can also be adjusted electrochemically. The large peak displacement of disulfide cleavage and formation, of ca. 1300 mV ($\Delta E \approx 30$ kcal mol^{-1}), indicates the bistability of the $(p\text{S-}\mathbf{1})_2/p\text{S-}\mathbf{1}^-$ couple over this potential range. Both forms can exist in this potential range under similar conditions, the nature of the species depending on the previous process [i.e., whether it was formed by oxidation or reduction (higher or lower electrochemical potential)]. This behaviour is closely related to the memory effect of bistable photochromic molecules, an important aspect in molecular data storage and molecular energy storage.

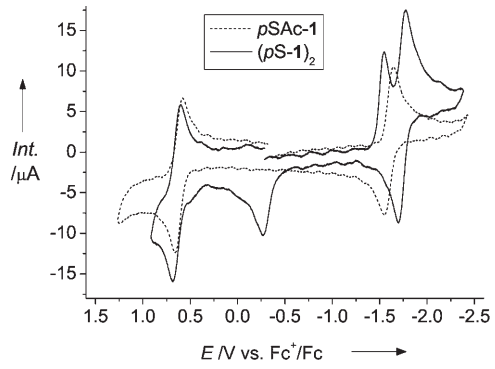

Figure 3. Cyclic voltammetry of $(p\text{S-}\mathbf{1})_2$ and *p*SAc-**1** in MeCN/0.2 M TBAH.

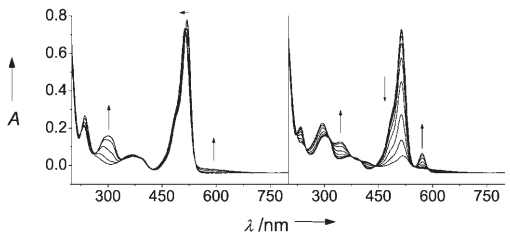

Figure 4. Spectroelectrochemistry of $(p\text{S-}\mathbf{1})_2$. First reduction (left) and second reduction to the typical BDP radical dianion (right) in MeCN/0.2 M TBAH.

The cyclic voltammogram of $(o\text{S-}\mathbf{1})_2$ is very similar to that of the *para* dimer, with the disulfide cleavage being facilitated by 45 mV (Table 3) because of steric crowding in the *ortho* derivative. Moreover, because of the close vicinity of the thiolate group formed in the first reduction, the second reduction on the BDP core is aggravated, occurring only at −1885 mV (Table 3). With regard to a possible chromophore–chromophore interaction in the ground state, the cyclic voltammogram of $(o\text{S-}\mathbf{1})_2$ [and also that of $(p\text{S-}\mathbf{1})_2$] does not show any splitting of the redox waves, thus stressing the conclusion implied by the similarity of the absorption spectra (i.e., both BDP moieties are independent and do not interact in the ground state).

Table 3. Electrochemical data of the compounds in MeCN/0.2 M TBAH.

	$E^{red}_{1/2}$ BDP [mV]	$E^{ox}_{1/2}$ BDP [mV]	E^{red}_p [mV]	E^{ox}_p [mV]
p-SAc-**1**	−1600	+620	–	–
$(p\text{S-}\mathbf{1})_2$	−1735	+645	−1545	−265
$(o\text{S-}\mathbf{1})_2$	−1885	+690	−1500	−235
1	−1630	+620	–	–

To obtain a better understanding of the ECE mechanism involved in the reduction of $(p\text{S-}\mathbf{1})_2$ to $p\text{S-}\mathbf{1}^-$ as described above, as well as the reoxidation process, the cyclic voltammogram of the *para* dimer was simulated[46] under the assumptions detailed in Scheme 4. Electron transfer to the diaryl disulfide subunit results in the dissociation of the disulfide bridge in the intermediately formed $(p\text{S-}\mathbf{1})_2^{-\cdot}$, yielding $p\text{S-}\mathbf{1}^-$ and the thio radical $p\text{S-}\mathbf{1}^{\cdot}$. Under the prevailing potential conditions, the latter species is instantly reduced to a second $p\text{S-}\mathbf{1}^-$, so that the net reaction of the first reduction is a transfer of two electrons. The corresponding formation of the disulfide bond (i.e., the formation of $(p\text{S-}\mathbf{1})_2$) proceeds in a first step from $p\text{S-}\mathbf{1}^-$ by oxidation to $p\text{S-}\mathbf{1}^{\cdot}$. Two of these radicals can then directly combine to yield $(p\text{S-}\mathbf{1})_2$, or $p\text{S-}\mathbf{1}^{\cdot}$ and $p\text{S-}\mathbf{1}^-$ can react to $(p\text{S-}\mathbf{1})_2^{-\cdot}$, which is then oxidized to the *para* dimer. The resulting calculated CV is compared to the experimentally measured cyclic voltammogram in Figure 5.

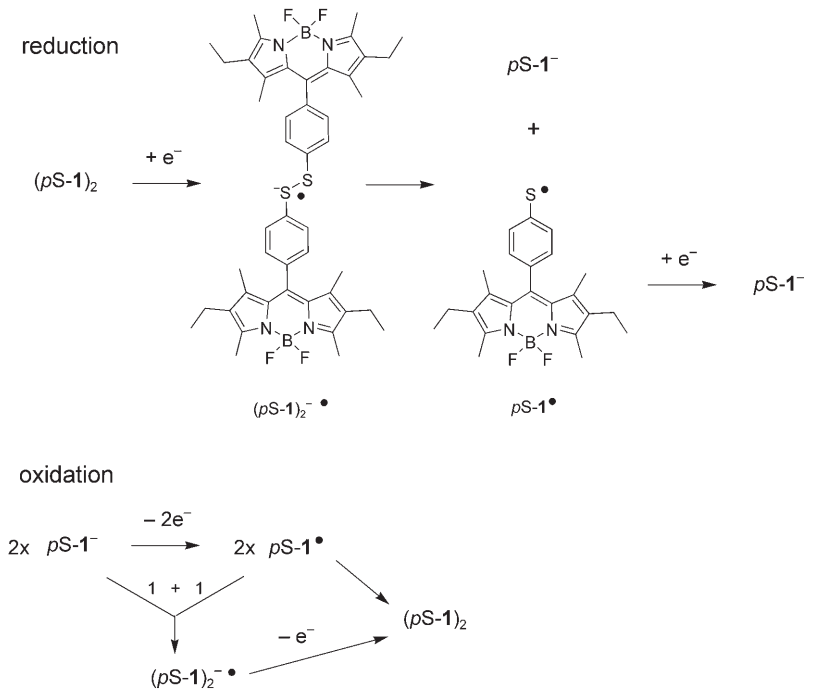

Scheme 4. ECE mechanism of the first reduction of $(p\text{S-}\mathbf{1})_2$ (top) and oxidation of $p\text{S-}\mathbf{1}^-$ with subsequent dimerization (bottom).

the instability of the species involved in the processes necessary to generate ECL.

Toward fluorescent tags: The validity of *p*-thiophenyl-substituted BDPs as both chemically and electrochemically addressable switches that can be conveniently operated in the visible spectral range having been established, recent progress in the redox labelling of proteins, as described in the Introduction, suggests that the thiol title compound *p*SH-**1** might be a versatile and promising candidate. In the manner reported above, the labelling reaction should be accomplishable by a redox step, with the optical spectroscopic features of the dye remaining largely unperturbed [i.e., the fluorescence properties should change in accordance with the

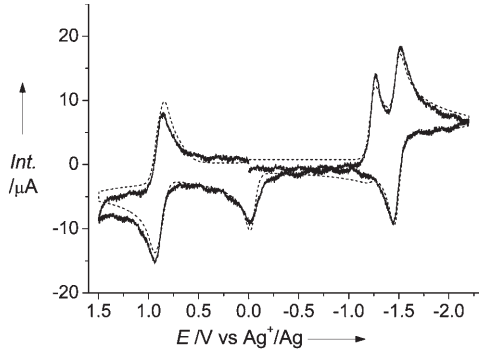

Figure 5. Simulated (dotted line) and measured (solid line) CVs of $(p\text{S-}\mathbf{1})_2$.

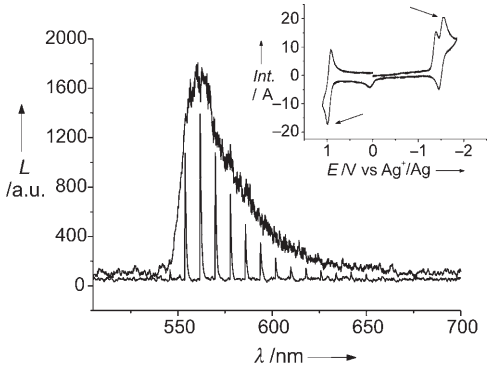

Figure 6. ECL spectra of $(p\text{S-}\mathbf{1})_2$ in CH_2Cl_2/0.2 M TBAH, with switch times of 1 s^{-1} (discrete lines) and 50 ms^{-1} (curve). Inset: corresponding CV, with the applied potentials indicated by the arrows.

Electrochemiluminescence: Keeping in mind that electroactive fluorophores are interesting candidates for several optoelectronic applications, mainly with respect to organic light-emitting devices (OLEDs), we investigated the electrochemiluminescence behaviour of *p*SAc-**1** and $(p\text{S-}\mathbf{1})_2$.[8c,21,47,48] By applying alternating potentials in the range of $E_p^{red/ox}$-(BDP), we obtained BDP-luminescence in both cases (illustrated for $(p\text{S-}\mathbf{1})_2$ in Figure 6).[49] Since the redox processes of the thiol/disulfide couple, for instance, are between the applied potential range for $(p\text{S-}\mathbf{1})_2$, one can assume that the excited state is generated by recombination of $p\text{S-}\mathbf{1}^{2-}$ and $(p\text{S-}\mathbf{1})_2{}^{2+}$, the mechanism being depicted in Scheme 5. The impact of the dye's structure is evident from the fact that we did not find ECL activity for $(o\text{S-}\mathbf{1})_2$, presumably because of step from *p*SH-**1** to $(p\text{S-}\mathbf{1})_2$]. Furthermore, the results presented above for $(o\text{S-}\mathbf{1})_2$ indicate that a typical BDP fluorescence of moderate intensity ($\Phi_f \approx 0.1$) could still be monitored even under high loading conditions, or if two labels were in close proximity. This is a valuable criterion for imaging applications. Additionally, in the case of *p*SH-**1**, two different steps could be invoked to remove background signals from unreacted stains: either conventional washing out of *p*SH-**1** or, through simple pH adjustment, easy and quantitative conversion of *p*SH-**1** into the fluorimetrically silent form $p\text{S-}\mathbf{1}^-$.

To test the suitability of this system for a broader range of labelling reactions, $p\text{S-}\mathbf{1}^-$ was coupled to cyanuric chloride to obtain a reactive BDP dye. Cyanuric chloride is widely

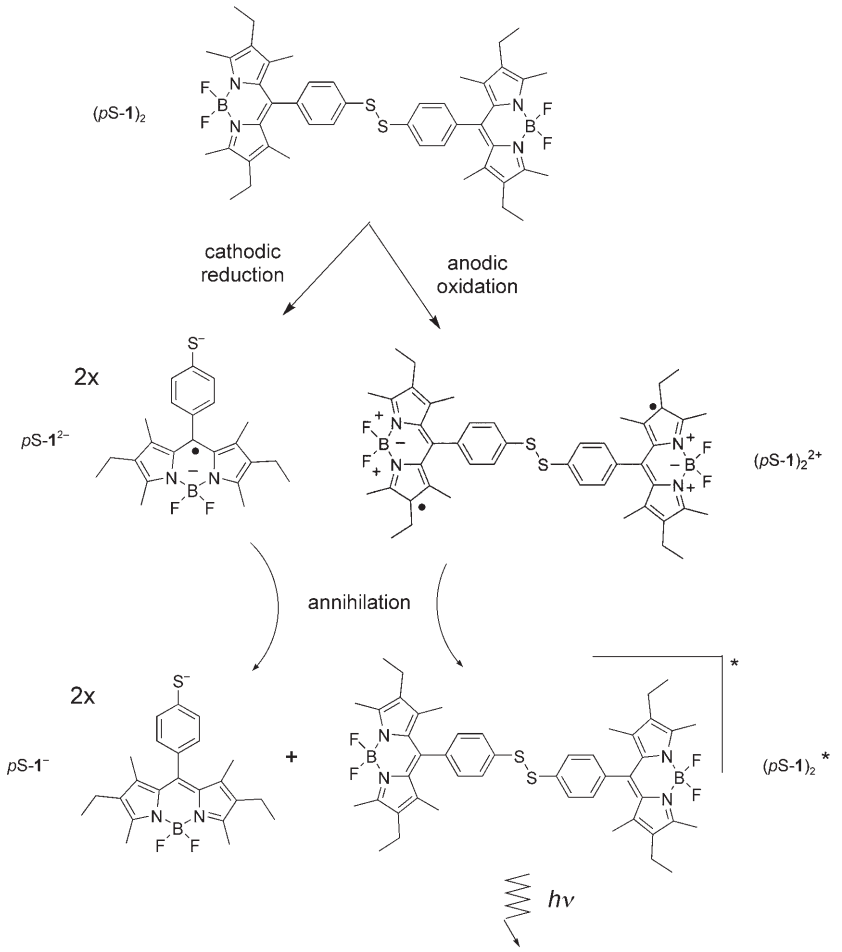

Scheme 5. Mechanism of ECL generation by annihilation in $(p\mathbf{S}\text{-}\mathbf{1})_2$. The involvement of $(p\mathbf{S}\text{-}\mathbf{1})_2^-$ as a minority electron donor cannot be ruled out.

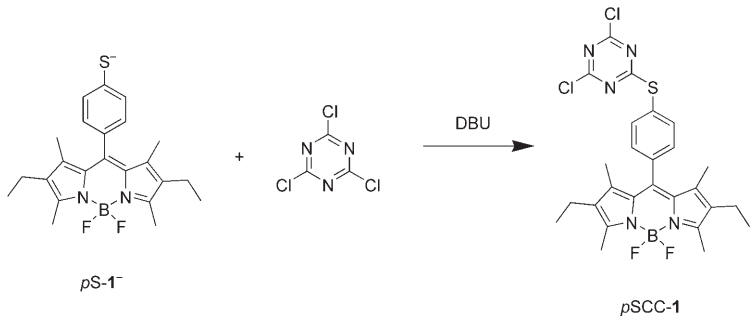

Scheme 6. Nucleophilic substitution of cyanuric chloride with $p\mathbf{S}\text{-}\mathbf{1}^-$.

used as a cross-linking agent for coloration—in the textile industry or for optical brighteners, for example—and has long been used as a linker for reactive fluorescent stains.[50] The reaction with *p*SH-**1** is straightforward and proceeds after base addition via the fluorimetrically silent $p\mathbf{S}\text{-}\mathbf{1}^-$ to yield *p*SCC-**1** as shown in Scheme 6. The exclusively formed monoproduct is highly fluorescent (i.e., the fluorescence of *p*SH-**1** is virtually revived during the reaction), and its typical BDP absorption band is bathochromically shifted by ca. 10 nm in relation to that of $p\mathbf{S}\text{-}\mathbf{1}^-$. Both dyes, *p*SH-**1** and *p*SCC-**1**, thus seem to show promise as fluorescent labels, and future work in our laboratories is currently being directed at detailed investigation of their staining properties.

Conclusion

This work offers a new concept of using the well investigated BDP core as a proton- and redox-addressable molecular switch, preserving all the favourable features of the family of BDP dyes while exhibiting full reversibility. With *p*SH-**1**, its deprotonated, fluorescently silent form $p\mathbf{S}\text{-}\mathbf{1}^-$ and the oxidized dimer $(p\mathbf{S}\text{-}\mathbf{1})_2$, the chemically and electrochemically switchable states of the system are introduced and characterized. By employing thiol/disulfide switching chemistry, it was possible to create a first molecular ensemble that shows both proton- and redox-controlled electrochemiluminescence. The potential fields of application of the versatile molecular system range from multimode molecular switching via chemically and/or redox-gated OLEDs to pH monitoring, protein labelling or other applications as a reactive dye. The *ortho* dimer $(o\mathbf{S}\text{-}\mathbf{1})_2$ allowed us to acquire deeper insight into structural requirements in redox switches, in the sense that excessive proximity of the redox centres precludes a potentially ECL-active chromophore from showing luminescence. On the other hand, the comparative investigation of the *ortho*- and the *para*-dimers revealed that a simple *meso*-*o*-thiophenyl group is a large enough spacer to prevent interchromophore communication of bichromophoric BDP dyes in the ground state, yet it retains the possibility for interaction in the excited state by energy transfer.

Experimental Section

General: Melting points were recorded on a Reichert-Thermovar micro melting apparatus and are not corrected. ^{1}H NMR and ^{13}C NMR spectra were measured on an Avance 300 instrument. Mass spectra were recorded on a Varian CH-5 and a Finnigan MAT 95 machine. IR spectra were obtained with a Biorad FTS 155 instrument in KBr disks.

Materials and synthesis: All solvents and chemicals were of reagent grade quality, were obtained commercially and were used without further purification except as noted below. The tetrabutylammonium hexafluorophosphate (TBAH) used as a supporting electrolyte and acetonitrile and dichloromethane for the electrochemical measurements were refined by previously described procedures.[51]

Compound *p*SAc-1: A mixture of 4-acetylsulfanylbenzoic acid[52] (200 mg, 1.0 mmol) in $SOCl_2$ (10.0 mL) was heated at reflux until a homogenous solution was obtained (1 h). Excess $SOCl_2$ was removed under vacuum. The remaining solid was dissolved in CH_2Cl_2 (100 mL) and 3-ethyl-2,4-dimethylpyrrole (0.3 mL, 285 mg, 2.34 mmol) was added. After the mixture had been heated at reflux for 4 h, $BF_3{\cdot}OEt_2$ and ethyl-diisopropyl-amine (3 mL of each) were added. After stirring for 30 min, the reaction mixture was quenched with water and extracted with CH_2Cl_2. The organic layer was dried over anhydrous Na_2SO_4 and evaporated. Column chromatography on silica gel with CH_2Cl_2/ethyl acetate (1:1) as an eluent gave *p*SAc-**1** as a red solid with a green lustre (9% yield, 40 mg, 0.09 mmol). M.p. > 222–223 °C; ^{1}H NMR (300 MHz, $CDCl_3$): δ = 7.55–7.52 (m, 2H), 7.37–7.33 (m, 2H), 2.53 (s, 6H; CH_3), 2.46 (s, 3H; CH_3), 2.30 (q, J = 7.6 Hz, 4H; CH_2), 1.33 (s, 6H; CH_3), 0.98 (t, J = 7.6 Hz, 6H; CH_3) ppm; ^{13}C NMR (75.5 MHz, $CDCl_3$): δ = 193.3 (q), 154.1 (q), 138.8 (q), 138.3 (q), 137.1 (q), 135.2 (+), 133.0 (q), 130.5 (q), 129.2 (+), 128.9 (q), 30.3 (+), 17.1 (−), 14.6 (+), 12.5 (+), 11.8 (+) ppm; FTIR (KBr): $\tilde{\nu}$ = 2968, 2926, 2856, 1717, 1536, 1474, 1320, 1193, 1119, 1065, 976, 760 cm^{-1}; MS (EI, 70 eV): *m/z*: 454 (100) $[M]^+$; HRMS (EI, 70 eV): calcd: 454.2066; found 454.2057.

Compound (*p*S-1)$_2$: A mixture of commercially available 4,4′-dithiobisbenzoic acid (500 mg, 1.6 mmol) in $SOCl_2$ (15.0 mL) was heated at reflux until a homogenous solution was obtained (30 h). Excess $SOCl_2$ was removed under vacuum. The remaining solid was dissolved in CH_2Cl_2 (200 mL), and 3-ethyl-2,4-dimethylpyrrole (0.8 mL, 760 mg, 6.24 mmol) was added. After the mixture had been heated at reflux for 4 h, $BF_3{\cdot}OEt_2$ and ethyl-diisopropyl-amine (3 mL each) were added. After stirring for 30 min, the reaction mixture was quenched with water and extracted with CH_2Cl_2. The organic layer was dried over anhydrous Na_2SO_4 and evaporated. Column chromatography on silica gel with CH_2Cl_2 as an eluent gave (*p*S-**1**)$_2$ as a red solid with a green lustre (11% yield, 150 mg, 0.18 mmol). M.p. > 265–267 °C; ^{1}H NMR (300 MHz, $CDCl_3$): δ = 7.63–7.60 (m, 4H), 7.27–7.24 (m, 4H), 2.52 (s, 12H; CH_3), 2.28 (q, J = 7.5 Hz, 8H; CH_2), 1.27 (s, 12H; CH_3), 0.96 (t, J = 7.5 Hz, 12H; CH_3) ppm; ^{13}C NMR (75.5 MHz, $CDCl_3$): δ = 154.1 (q), 138.8 (q), 138.0 (q), 137.5 (q), 135.2 (q), 133.0 (q), 130.6 (q), 129.2 (+), 128.6 (+), 17.0 (−), 14.6 (+), 12.5 (+), 11.8 (+) ppm; FTIR (KBr): $\tilde{\nu}$ = 2964, 2929, 1544, 1474, 1320, 1193, 1073, 980 cm^{-1}; MS (FD, 70 eV): *m/z*: 822 (100) $[M]^+$; HRMS (EI, 70 eV): calcd: 822.3771; found 822.3767.

Compound *p*SH-1: A mixture of (*p*S-**1**)$_2$ (60 mg, 0.07 mmol) and Zn (2.0 g) was stirred in AcOH (20.0 mL). After ca. 2.5 h, excessive Zn was removed by filtration, and water was added to the remaining solution. After extraction with CH_2Cl_2, the organic layer was dried over anhydrous Na_2SO_4 and evaporated. Column chromatography on silica gel with CH_2Cl_2 as an eluent gave *p*SH-**1** as a red solid with a green lustre (50% yield, 30 mg, 0.07 mmol). M.p. > 210–212 °C; ^{1}H NMR (300 MHz, $CDCl_3$): δ = 7.39–7.37 (m, 2H), 7.16–7.13 (m, 2H), 3.59 (s, 1H), 2.52 (s, 6H; CH_3), 2.30 (q, J = 7.5 Hz, 4H; CH_2), 1.33 (s, 6H; CH_3), 0.98 (t, J = 7.5 Hz, 6H; CH_3) ppm; ^{13}C NMR (75.5 MHz, $CDCl_3$): δ = 153.9 (q), 139.3 (q), 138.3 (q), 133.1 (q), 132.9 (q), 132.1 (q) 130.8 (q), 129.7 (+), 129.1 (+), 17.1 (−), 14.6 (+), 12.5 (+), 11.9 (+) ppm; FTIR (KBr): $\tilde{\nu}$ = 2968, 2929, 1532, 1474, 1316, 1185, 1069, 976, 803 cm^{-1}; MS (DCI, NH_3): *m/z*: 412 (100) $[M]^+$; HRMS (EI, 70 eV): calcd: 412.1949; found 412.1960.

Compound (*o*S-1)$_2$: A mixture of commercially available 2,2′-dithiobisbenzoic acid (500 mg, 1.6 mmol) in $SOCl_2$ (15.0 mL) was heated at reflux until a homogenous solution was obtained (18 h). Excess $SOCl_2$ was removed under vacuum. The remaining solid was dissolved in CH_2Cl_2 (200 mL), and 3-ethyl-2,4-dimethylpyrrole (0.8 mL, 760 mg, 6.24 mmol) was added. After the mixture had been heated at reflux for 4 h, $BF_3{\cdot}OEt_2$ and ethyl-diisopropyl-amine (3 mL each) were added. After stirring for 30 min, the reaction mixture was quenched with water and extracted with CH_2Cl_2. The organic layer was dried over anhydrous Na_2SO_4 and evaporated. Column chromatography on silica gel with CH_2Cl_2 as an eluent gave (*o*S-**1**)$_2$ as a red solid with a green lustre (11% yield, 150 mg, 0.18 mmol). M.p. > 360 °C; ^{1}H NMR (300 MHz, $CDCl_3$): δ = 7.67–7.62 (m, 2H), 7.20–7.16 (m, 4H), 2.52 (s, 12H; CH_3), 2.31 (q, J = 7.6 Hz, 8H; CH_2), 1.25 (s, 12H; CH_3), 1.00 (t, J = 7.6 Hz, 12H; CH_3) ppm; ^{13}C NMR (75.5 MHz, $CDCl_3$): δ = 154.6 (q), 137.9 (q), 136.1 (q), 136.0 (q), 133.6 (q), 133.0 (q), 130.4 (q), 129.7 (+), 129.1 (+), 17.1 (−), 14.6 (+), 12.6 (+), 11.2 (+) ppm; FTIR (KBr): $\tilde{\nu}$ = 2964, 2926, 1544, 1478, 1320, 1192, 1073, 980 cm^{-1}; MS (FD, 70 eV): *m/z*: 822 (100) $[M]^+$; HRMS (EI, 70 eV): calcd: 822.3771; found 822.3770.

Compound 1: This was synthesized as reported by us previously.[17a]

Steady-state absorption and fluorescence spectroscopy: Steady-state absorption measurements were carried out on a Bruins Instruments Omega 10 and a Cary 5000 UV/Vis/NIR spectrophotometer. The steady-state fluorescence spectra were recorded with a Spectronics Instrument 8100 spectrofluorimeter. For all measurements, the temperature was kept constant at 298 ± 2 K. Unless otherwise noted, only dilute solutions of an optical density of less then 0.1 at the absorption maximum were used. Fluorescence experiments were performed with a 90° standard geometry, with polarizers set at 54.7° for emission and 0° for excitation. The fluorescence quantum yields (Φ_f) were determined relative to fluorescein 27 in 0.1 N NaOH (Φ_f = 0.90 ± 0.03).[53] All the fluorescence spectra presented here were corrected for the spectral response of the detection system (calibrated quartz halogen lamp placed inside an integrating sphere; Gigahertz-Optik) and for the spectral irradiance of the excitation channel (calibrated silicon diode mounted at a sphere port; Gigahertz-Optik). The uncertainties of the fluorescence quantum yields were determined to ±5% (for $\Phi_f > 0.2$) and ±10% (for $0.2 > \Phi_f > 0.02$).

Spectral fitting procedure: The full widths at half-maximum (*fwhm*s) of the reported absorption and emission bands were calculated from the deconvoluted absorption and emission spectra, respectively, which had been converted to the energy scale and subsequently fitted by a Gaussian fit. Independent of the compound, five components were necessary in both absorption and fluorescence spectra to yield acceptable fitting results with regard to the lowest energy transition. The *fwhm*s of the components were linked and no other constrains were set.

Time-resolved fluorescence spectroscopy: Fluorescence lifetimes (τ_f) were determined by a unique customized laser impulse fluorimeter with picosecond time resolution, which we have described in earlier publications.[18b,54] The fluorescence was collected at right angles (polarizer set at 54.7°; monochromator with spectral bandwidths of 4, 8 and 16 nm) and the fluorescence decays were recorded with a modular single-photon timing unit as described in reference [18b]. While producing typical instrumental response functions of *fwhm* of ca. 25–30 ps, the time division was 4.8 ps per channel and the experimental accuracy amounted to ±3 ps. The laser beam was attenuated with a double prism attenuator (LTB) and typical excitation energies were in the nanowatt to microwatt range (average laser power). The fluorescence lifetime profiles were analysed on a PC with the Global Unlimited V2.2 software package (Laboratory for Fluorescence Dynamics, University of Illinois). The goodness of fit of the single decays as judged by reduced chi-squared (χ_R^2) and the autocorrelation function *C(j)* of the residuals was always below $\chi_R^2 < 1.2$. For all the dyes, decays were recorded at three different emission wavelengths over the BDP-type emission spectrum and were analysed globally. Such a global analysis of decays recorded at different emission wavelengths implies that the decay times of the species are linked while the program varies the preexponential factors and lifetimes until the changes in the error surface (χ^2 surface) are minimal; that is, convergence is reached. The fitting results are judged for every single decay (local χ_R^2)

and for all the decays (global χ_R^2). The errors for all the global analytical results presented here were below a global $\chi_R^2 = 1.2$.

Lifetime distribution analysis (LDA): LDA of the fluorescence decay traces that could not be sufficiently described by one or two exponentials in the global analysis was performed with the FLA900 software package (Edinburgh Analytical Instruments, level 2, version 1.6). The lifetime range was set to a reasonable value, the starting channel shift was set to 0.5 (not fixed), all available channels were used, and the maximum possible number of 100 individual exponential lifetimes was employed. No other constraints were made. The quality of the fit was again reviewed by the χ^2 analysis. For all results χ^2 was below 1.3.

Cyclic voltammetry, spectroelectrochemistry, electrochemiluminescence: CV measurements were performed with solutions of the appropriate compound (ca. 1 mM) in highly pure solvents buffered with TBAH (0.2 M, vide ante) on a potentiostat/galvanostat (EG&G 283A). The measurement cell had a three-electrode set-up (Pt working electrode, gold counter-electrode and Ag/AgCl pseudo-reference electrode) and the measurements were referenced against ferrocenium/ferrocene (Fc^+/Fc) as the internal standard. A Perkin–Elmer Lambda 9 UV/Vis/NIR spectrophotometer in combination with an Amel 2053 potentiostat/galvanostat and a custom-build quartz cuvette with a minigrid gold net as transparent working electrode was employed for the spectroelectrochemical experiments (for a detailed description see reference [55]). ECL measurements were carried out on a Hitachi F-4500 fluorimeter fitted with a customized ECL cell and a set-up as described in reference [56]. For the ECL experiments, solvents of similar grade to those used in the other electrochemical studies were employed, and the concentrations of the compounds were adjusted to about 1 mM. TBAH (0.2 M) served as supporting electrolyte, and the measurements were performed without stirring of the solutions. The potential was switched with alternation between the oxidation and reduction potentials (see inset of Figure 6, electrochemical switching frequency 1 s^{-1}, scan rate of the spectrometer 240 nm min^{-1}). The spiked spectrum is the result of the "slow" switching frequency of 1 s^{-1}, whilst the other spectra were obtained with $\nu = 50$ and 20 ms^{-1} in the case of *p*SAc-**1** and (*p*S-**1**)$_2$.

Acknowledgment

Financial support by the German Research Foundation (DFG), the German National Academic Foundation (C.T.) and BAM's Ph.D. programme (H.R.) is greatly appreciated. This work is part of the Graduate College "Sensory Photoreceptors in Natural and Artificial Systems" granted by the DFG (GRK 640, University of Regensburg).

[1] a) L. Pu, *Chem. Rev.* **2004**, *104*, 1687–1716; b) A. P. de Silva, B. McCaughan, B. O. F. McKinney, M. Querol, *Dalton Trans.* **2003**, 1902–1913; c) R. Martinez-Manez, F. Sancenon, *Chem. Rev.* **2003**, *103*, 4419–4476.

[2] a) F. M. Raymo, M. Tomasulo, *Chem. Soc. Rev.* **2005**, *34*, 327–336; b) *Molecular Switches* (Ed.: B. Feringa), Wiley-VCH, Weinheim, **2002**; c) A. P. de Silva, D. B. Fox, T. S. Moody, S. M. Weir, *Trends Biotechnol.* **2001**, *19*, 29–34.

[3] a) A. P. de Silva, N. D. McClenaghan, *Chem. Eur. J.* **2003**, *10*, 574–586; b) V. Balzani, A. Credi, M. Venturi, *Chem. Phys. Chem.* **2003**, *3*, 49–59; c) F. M. Raymo, *Adv. Mater.* **2002**, *14*, 401–414.

[4] a) Special Issue (6) on "Molecular Machines" *Acc. Chem. Res.* **2001**, *34*, 409–522; b) C. P. Mandl, B. König, *Angew. Chem.* **2004**, *116*, 1650–1652; *Angew. Chem. Int. Ed.* **2004**, *43*, 1622–1624; c) *Molecular Devices and Machines, A Journey into the Nanoworld* (Eds.: V. Balzani, M. Venture, A. Credi), Wiley-VCH, Weinheim, **2003**; d) A. R. Pease, J. F. Stoddart, *Struct. Bonding* **2001**, *99*, 189–236.

[5] a) J. R. Heath, *Pure Appl. Chem.* **2000**, *72*, 11–20; b) D. T. McQuade, A. E. Pullen, T. M. Swager, *Chem. Rev.* **2000**, *100*, 2537–2574; c) A. Harriman, R. Ziessel, *Chem. Commun.* **1996**, 1707–1716.

[6] a) T. G. Goodson, III, *Acc. Chem. Res.* **2005**, *38*, 99–107; b) J. M. J. Frechet, *J. Polym. Sci. Part A: Polym. Chem.* **2003**, *41*, 3713–3725; c) V. Balzani, P. Ceroni, M. Maestri, C. Saudan, V. Vicinelli, *Top. Curr. Chem.* **2003**, *228*, 159–191; d) M. A. Miller, R. K. Lammi, S. Prathapan, D. Holten, J. S. Lindsey, *J. Org. Chem.* **2000**, *65*, 6634–6649; e) A. Burghart, L. H. Thoresen, J. Chen, K. Burgess, F. Bergström, L. B.-Å. Johansson, *Chem. Commun.* **2000**, 2203–2204; f) J. Y. Ju, A. N. Glazer, R. A. Mathies, *Nucleic Acids Res.* **1996**, *24*, 1144–1148.

[7] a) G. M. Tsivgoulis, J.-M. Lehn, *Adv. Mater.* **1997**, *9*, 627–630; b) H. Spreitzer, J. Daub, *Chem. Eur. J.* **1996**, *2*, 1150–1158; c) J. Daub, C. Fischer, J. Salbeck, K. Ulrich, *Adv. Mater.* **1990**, *2*, 366–369.

[8] a) K. Rurack, M. Kollmannsberger, J. Daub, *Angew. Chem.* **2001**, *113*, 396–399; *Angew. Chem. Int. Ed.* **2001**, *40*, 385–387; b) G. Hennrich, H. Sonnenschein, U. Resch-Genger, *J. Am. Chem. Soc.* **1999**, *121*, 5073–5074; c) M. Kollmannsberger, T. Gareis, S. Heinl, J. Breu, J. Daub, *Angew. Chem.* **1997**, *109*, 1391–1393; *Angew. Chem. Int. Ed. Engl.* **1997**, *36*, 1333–1335.

[9] a) L. Gobbi, P. Seiler, F. Diederich, V. Gramlich, C. Boudon, J.-P. Gisselbrecht, M. Gross, *Helv. Chim. Acta* **2001**, *84*, 743–777; b) L. Gobbi, P. Seiler, F. Diederich, *Angew. Chem.* **1999**, *111*, 737–740; *Angew. Chem. Int. Ed. Engl.* **1999**, *38*, 674–678.

[10] a) C. Trieflinger, K. Rurack, J. Daub, *Angew. Chem.* **2005**, *117*, 2328–2331; *Angew. Chem. Int. Ed.* **2005**, *44*, 2288–2291; b) J. Achatz, C. Fischer, J. Salbeck, J. Daub, *J. Chem. Soc. Chem. Commun.* **1991**, 504–507.

[11] A number of redox-active thiol/disulfide switches that can be probed by various other instrumental methods have been reported; see, for example: a) H. Graubaum, F. Tittelbach, G. Lutze, K. Gloe, M. Mackrodt, *J. Prakt. Chem.* **1997**, *339*, 55–58; b) M. Irie, O. Miyatake, K. Uchida, T. Eriguchi, *J. Am. Chem. Soc.* **1994**, *116*, 9894–9900; c) S. Shinkai, K. Inuzuka, O. Miyazaki, O. Manabe, *J. Org. Chem.* **1984**, *49*, 3440–3442; d) S. Shinkai, K. Inuzuka, O. Manabe, *Chem. Lett.* **1983**, 747–750; e) T. Minami, S. Shinkai, O. Manabe, *Tetrahedron Lett.* **1982**, *23*, 5167–5170. An example of a thiol/disulfide-controlled molecular machine based on rotaxanes has also been published recently, f) Y. Furusho, T. Hasegawa, A. Tsuboi, N. Kihara, T. Takata, *Chem. Lett.* **2000**, 18–19.

[12] a) A. P. Fernandes, A. Holmgren, *Antioxid. Redox Signal.* **2004**, *6*, 63–74; b) D. Barford, *Curr. Opin. Struct. Biol.* **2004**, *14*, 679–686; c) K. Linke, U. Jakob, *Antioxid. Redox Signal.* **2003**, *5*, 425–434; d) H. Sies, *Free Radic. Biol. Med.* **1999**, *27*, 916–921.

[13] a) G. T. Hanson, R. Aggeler, D. Oglesbee, M. Cannon, R. A. Capaldi, R. Y. Tsien, S. J. Remington, *J. Biol. Chem.* **2004**, *279*, 13044–13053; b) H. Østergaard, A. Henriksen, F. G. Hansen, J. R. Winther, *EMBO J.* **2001**, *20*, 5853–5862.

[14] H. Østergaard, C. Tachibana, J. R. Winther, *J. Cell Biol.* **2004**, *166*, 337–345.

[15] a) T. Sakata, Y. Yan, G. Marriott, *J. Org. Chem.* **2005**, *70*, 2009–2013; b) P. Ge, P. R. Selvin, *Bioconjugate Chem.* **2003**, *14*, 870–876.

[16] R. Rinaldi, G. Maruccio, A. Biasco, P. Visconti, V. Arima, R. Cingolani, *Ann. N.Y. Acad. Sci.* **2003**, *1006*, 187–197.

[17] a) P. Toele, H. Zhang, C. Trieflinger, J. Daub, M. Glasbeek, *Chem. Phys. Lett.* **2003**, *368*, 66–75; b) M. Kollmannsberger, K. Rurack, U. Resch-Genger, J. Daub, *J. Phys. Chem. A* **1998**, *102*, 10211–10220; c) J. Karolin, L. B.-A. Johansson, L. Strandberg, T. Ny, *J. Am. Chem. Soc.* **1994**, *116*, 7801–7806; d) J. A. Pardoen, J. Lugtenburg, G. W. Canters, *J. Phys. Chem.* **1985**, *89*, 4272–4277.

[18] a) W. Zhao, E. M. Carreira, *Angew. Chem.* **2005**, *117*, 1705–1707; *Angew. Chem. Int. Ed.* **2005**, *44*, 1677–1679; b) Z. Shen, H. Röhr, K. Rurack, H. Uno, M. Spieles, B. Schulz, G. Reck, N. Ono, *Chem. Eur. J.* **2004**, *10*, 4853–4871; c) K. Rurack, M. Kollmannsberger, J. Daub, *New J. Chem.* **2001**, *25*, 289–292; d) H. Kim, A. Burghart, M. B. Welch, J. Reibenspies, K. Burgess, *Chem. Commun.* **1999**, 1889–1890; e) J. Chen, J. Reibenspies, A. Derecskei-Kovacs, K. Burgess, *Chem. Commun.* **1999**, 2501–2502.

[19] a) Y. Gabe, Y. Urano, K. Kikuchi, H. Kojima, T. Nagano, *J. Am. Chem. Soc.* **2004**, *126*, 3357–3367; b) C. Goze, G. Ulrich, L. Charbonnière, M. Cesario, T. Prangé, R. Ziessel, *Chem. Eur. J.* **2003**, *9*,

3748–3755; c) R. W. Wagner, J. S. Lindsey, *Pure Appl. Chem.* **1996**, *68*, 1373–1380.
[20] a) G. Beer, K. Rurack, J. Daub, *Chem. Commun.* **2001**, 1138–1139; b) G. Beer, C. Niederalt, S. Grimme, J. Daub, *Angew. Chem.* **2000**, *112*, 3385–3388; *Angew. Chem. Int. Ed.* **2000**, *39*, 3252–3255; c) M. Kollmannsberger, K. Rurack, U. Resch-Genger, W. Rettig, J. Daub, *Chem. Phys. Lett.* **2000**, *329*, 363–369.
[21] a) J. M. Brom, Jr., J. L. Langer, *J. Alloys Compd.* **2002**, *338*, 112–115; b) R. Y. Lai, A. J. Bard, *J. Phys. Chem. B* **2003**, *106*, 5036–5042.
[22] a) L. Milanesi, G. D. Reid, G. S. Beddard, C. A. Hunter, J. P. Waltho, *Chem. Eur. J.* **2004**, *10*, 1705–1710; b) W. M. Macindoe, A. H. van Oijen, G.-J. Boons, *Chem. Commun.* **1998**, 847–848.
[23] F. Bergström, I. Mikhalyov, P. Hägglöf, R. Wortmann, T. Ny, L. B.-Å. Johansson, *J. Am. Chem. Soc.* **2002**, *124*, 196–204.
[24] Various attempts to obtain the corresponding monomer *o*SH-**1** from (*o*S-**1**)$_2$ failed, and cyclovoltammetric measurements suggested that the close vicinity of nucleophilic thiol group and BDP residue most probably renders the monomer rather unstable.
[25] Y. Fujimoto, N. Katayama, Y. Ozaki, S. Yasui, K. Iriyama, *J. Mol. Struct.* **1992**, *274*, 183–195.
[26] K. Rurack, M. Kollmannsberger, U. Resch-Genger, J. Daub, *J. Am. Chem. Soc.* **2000**, *122*, 968–969.
[27] T. Gareis, C. Huber, O. S. Wolfbeis, J. Daub, *Chem. Commun.* **1997**, 1717–1718.
[28] Because of the sensitivity of such thiolates towards oxidation, these measurements were performed under Ar. Note that the use of such conditions has a negligible influence on the fluorescence features of the title dyes: $\Phi_f = 0.64$ and 0.65 for *p*SH-**1** in aerated and de-aerated MeCN, for example.
[29] W. Rettig, *Top. Curr. Chem.* **1994**, *169*, 253–299.
[30] AMPAC V6.55, Semichem, Inc. M. J. S. Dewar, E. G. Zoebisch, E. F. Healy, J. J. P. Stewart, *J. Am. Chem. Soc.* **1985**, *107*, 3902–3909.
[31] Such a dependence of the intensity of the bathochromically shifted transition on the interannular twist angle has also been found for the phenolate anion of 9-(*p*-hydroxyphenyl)acridine, V. Zanker, A. Reichel, *Z. Elektrochem.* **1959**, *63*, 1133–1140 and V. Zanker, A. Reichel, *Z. Elektrochem.* **1960**, *64*, 431–437.
[32] a) Y. Wang, C.-P. Chang, H. Tian, *Dyes Pigm.* **2002**, *54*, 265–274; b) Y. Wang, C.-P. Chang, Y. Wu, H. Tian, *Dyes Pigm.* **2001**, *51*, 127–136.
[33] The findings that both the absorption and emission bands of (*o*S-**1**)$_2$ are only slightly broader (on average by $\approx 15\,cm^{-1}$) than those of (*p*S-**1**)$_2$ suggest that exciton coupling such as has been observed for π-conjugated pre-twisted BDPs by Falk and Schoppel (see ref. [39]) does not play a major role in the present case.
[34] R. F. Khairutdinov, N. Serpone, *J. Phys. Chem. B* **1997**, *101*, 2602–2610.
[35] W. R. Ware in *Photochemistry in Organized and Constrained Media* (Ed.: V. Ramamurthy), VCH, New York, **1991**, pp. 563–602.
[36] a) K. Rurack, K. Hoffmann, W. Al-Soufi, U. Resch-Genger, *J. Phys. Chem. B* **2002**, *106*, 9744–9752; b) R. Fritz, A. Kungl, W. Rettig, J. Springer, *Chem. Phys. Lett.* **1996**, *260*, 409–417; c) F. V. Bright, G. C. Catena, J. Huang, *J. Am. Chem. Soc.* **1990**, *112*, 1343–1346.
[37] D. R. James, Y.-S. Liu, P. De Mayo, W. R. Ware, *Chem. Phys. Lett.* **1985**, *120*, 460–465.
[38] S. G. Tarasov, J. R. Casas-Finet, W. M. Cholody, C. J. Michejda, *Photochem. Photobiol.* **1999**, *70*, 568–578.
[39] H. Falk, G. Schoppel, *Monatsh. Chem.* **1990**, *121*, 67–76.
[40] F. Li, S. I. Yang, Y. Ciringh, J. Seth, I. C. H. Martin, D. L. Singh, D. Kim, R. R. Birge, D. F. Bocian, D. Holten, J. S. Lindsey, *J. Am. Chem. Soc.* **1998**, *120*, 10001–10017.
[41] Note that the involvement of triplet states in the deactivation of the BDP's S_1 state was found to be of negligible importance (e.g. refs. [17a, 18b], J. Banuelos Prieto, F. López Arbeloa, V. Martinez-Martinez, I. López Arbeloa, *Chem. Phys.* **2004**, *296*, 13–22) and significantly lower than in rhodamine dyes; see, for example, F. Liang, H. P. Zeng, Z. R. Sun, Y. Z. Yuan, Z. G. Yao, Z. Z. Xu, *J. Opt. Soc. Am. B* **2001**, *18*, 1841–1845.
[42] Corresponding data in CH_2Cl_2: −1750 mV and +580 mV versus Fc^+/Fc.
[43] These two processes belong together as confirmed by multisweep experiments under thin-film conditions. The corresponding data in CH_2Cl_2 are −1750 mV and +590 mV; the BDP's redox potentials of (*p*S-**1**)$_2$ lie at −1875 mV and +590 mV in CH_2Cl_2.
[44] S. Antonello, K. Daasbjerg, H. Jensen, F. Taddei, F. Maran, *J. Am. Chem. Soc.* **2003**, *125*, 14905–14916.
[45] Diaryl disulfides are known to be reductively cleaved to thiolate anions, see refernce [44] and references therein.
[46] By use of the Digisim 3.03a program; M. Rudolph, S. W. Feldberg, *Digisim 3.03a*, Bioanalytical Systems, Inc., West Lafayette, IN, USA, **1994–2000**.
[47] a) K. Kelnhofer, A. Knorr, Y. H. Tak, H. Bässler, J. Daub, *Acta Polym.* **1997**, *48*, 188–192; b) J. Daub, K. Kelnhofer, T. Gareis, A. Knorr, M. Kollmannsberger, Y.-H. Tak, H. Bässler, *Polym. Preprints* **1997**, *38*, 339–340; c) J. Strauss, J. Daub, *Adv. Mater.* **2002**, *14*, 1652–1655; d) J. Strauss, J. Daub, *Adv. Mater.* **2003**, *15*, 258; e) C. Trieflinger, H. Röhr, K. Rurack, J. Daub, *Angew. Chem.* **2005**, *117*, DOI: 10.1002/ange. 200501573; *Angew. Chem. Int. Ed.* **2005**, *44*, DOI: 10.1002/anie.200501573.
[48] M. M. Richter, *Chem. Rev.* **2004**, *104*, 3003–3036.
[49] The bathochromic shift of ca. 20 nm between the fluorescence and the ECL spectrum is well known and can be attributed to reabsorption effects due to the higher dye concentration used in the ECL experiment and to the different dielectric properties of the supporting electrolyte.
[50] a) C. Kempter, W. Pötter, N. Binding, H. Kläning, U. Witting, U. Karst, *Anal Chim. Acta* **2000**, *410*, 47–64; b) D. Blakeslee, M. G. Baines, *J. Immunol. Methods* **1976**, *13*, 305–320; c) *Reactive Dyes in Protein and Enzyme Technology* (Eds. Y. D. Clonis, A. Atkinson, C. J. Bruton, C. R. Lowe), Macmillan, Basingstoke, UK, **1987**.
[51] a) J. Salbeck, Dissertation, Universität Regensburg, **1988**; b) J. Salbeck, *J. Electroanal. Chem.* **1993**, *340*, 169–175.
[52] Synthesized according to P. R. Menard, J. T. Suh, H. Jones, B. Love, E. S. Neiss, J. Wilde, A. Schwab, W. S. Mann, *J. Med. Chem.* **1985**, *28*, 328–332.
[53] J. Olmsted, III, *J. Phys. Chem.* **1979**, *83*, 2581–2584.
[54] U. Resch, K. Rurack, *Proc. SPIE-Int. Soc. Opt. Eng.* **1997**, *3105*, 96–103.
[55] J. Salbeck, *Anal. Chem.* **1993**, *65*, 2169–2173, M. Bueschel, C. Stadler, C. Lambert, M. Beck, J. Daub, *J. Electroanal. Chem.* **2000**, *484*, 24–32.
[56] S. Hien, Ph.D. Thesis, University of Regensburg, **1995**.

Received: June 24, 2005
Published online: October 17, 2005

